

# Se-loss-induced CIS Thin Films in RTA Process after Co-sputtering Using CuSe<sub>2</sub> and InSe<sub>2</sub> Targets

Nam-Hoon Kim\*, Young-Kil Jun\* and Geum-Bae Cho<sup>†</sup>

**Abstract** – Chalcopyrite CuInSe<sub>2</sub> (CIS) thin films were prepared without Se- / S-containing gas by co-sputtering using CuSe<sub>2</sub> and InSe<sub>2</sub> selenide-targets and rapid thermal annealing. The grain size increased to a maximum of 54.68 nm with a predominant (112) plane. The tetragonal distortion parameter  $\eta$  decreased and the inter-planar spacing  $d_{(112)}$  increased in the RTA-treated CIS thin films annealed at a 400°C, which indicates better crystal quality. The increased carrier concentration of RTA-treated p-type CIS thin films led to a decrease in resistivity due to an increase in Cu composition at annealing temperatures  $\geq 350^\circ\text{C}$ . The optical band gap energy ( $E_g$ ) of CIS thin films decreased to 1.127 eV in RTA-treated CIS thin films annealed at 400°C due to the improved crystallinity, elevated carrier concentration and decreased In composition.

**Keywords:** Thin Film, CuSe<sub>2</sub> and InSe<sub>2</sub> Targets, Co-sputtering, RTA

## 1. Introduction

Copper Indium Diselenide (CIS) is an I-III-IV<sub>2</sub> chalcopyrite semiconductor that is used as an absorber layer in heterostructured thin film photovoltaic devices. The material has a high absorption coefficient ( $\alpha > 10^5 \text{ cm}^{-1}$ ) and direct band gap energy ( $E_g \sim 1.04 \text{ eV}$ ) [1], which makes it suitable for high-efficiency thin film solar cell applications. Several methods have been used and developed to prepare CIS thin films. A co-evaporation method followed by post-selenization process is used widely to achieve high-level conversion efficiency [2, 3]. Selenization / sulfurization of the sputtered Cu-In precursors using Se- / S-containing vapor is a suitable method for preparing CIS thin films at low cost [4]. On the other hand, these methods have several critical disadvantages in selenization / sulfurization processes for industrial production. The major drawbacks were highly toxic gas, process complexity with expensive equipment, slow reaction rate and poor adhesion to the back contact and poor reproducibility [5-7]. An eco-friendly, simple and cheap method for fabricating CIS thin films without additional selenization / sulfurization process using Se- / S-containing vapor needs to be developed, but few studies have been performed. Several efforts have been made to develop this method for preparing CIS thin films, such as Cu<sub>2</sub>Se + In<sub>2</sub>Se<sub>3</sub> by Chen and CuSe<sub>2</sub>+In in a previous study [8]. However, the loss of Se in thin films due to volatilization in heat treatment at higher temperatures for longer times could not be suppressed [9, 10]. In this study, CuSe<sub>2</sub> and InSe<sub>2</sub> selenides as the starting targets for co-

sputtering were used to prepare CIS thin films by adjusting the chemical composition ratio of Se in the thin films. Rapid thermal annealing (RTA) is a powerful annealing method with a short cycle time and reduced thermal exposure [11]. The RTA was used in N<sub>2</sub> gas ambient to form polycrystalline chalcopyrite phases and control Se-loss from the Se-rich thin films with changes in the annealing temperature. This study examined the microstructure, electrical and optical properties of the Se-loss-induced near-stoichiometric CIS thin films from Se-rich thin films.

## 2. Experimental Details

Corning glass (20×20 mm<sup>2</sup>) was used as a substrate for deposition of 530-nm thin films by RF magnetron co-sputtering (IDT Engineering Co.). Commercial CuSe<sub>2</sub> (TASCO, 99.99% purity, 2 inches-diameter) and InSe<sub>2</sub> (LTS Chemical Inc., 99.99% purity, 2 inches-diameter) targets were used at RF sputtering powers of 80 W and 50 W, respectively. The fixed set of process parameters was followed: pre-sputtering for 3 minutes, Ar gas flux of 50 sccm, base pressure of  $1.0 \times 10^{-6}$  Torr, 5.0 cm distance from the substrate to targets and vacuum pressure of  $7.5 \times 10^{-3}$  Torr during the sputtering process for 23 minutes at room temperature. The total thickness of the co-sputtered CuSe<sub>2</sub> and InSe<sub>2</sub> thin films was approximately 530 nm, which had the same deposition rate of 11.5 nm/min for each target. The RTA (Modular Process Technology Co., RTP-600S) treatment of the 530-nm-thick thin films was performed to improve the temperature uniformity over the conventional furnace for 1 minute in N<sub>2</sub> gas ambient at various temperatures ranging from 250°C to 400°C with an interval of 50°C [9, 10]. A non-selenization / non-

<sup>†</sup> Corresponding Author: Dept. of Electrical Engineering, Chosun University, Korea. (gbcho@chosun.ac.kr)

\* Dept. of Electrical Engineering, Chosun University, Korea. (nhkim@chosun.ac.kr)

Received: December 3, 2013; Accepted: March 19, 2014

sulfurization process was performed during the RTA treatment for preparing CIS thin films without additional Se- / S-containing gas. The microstructure of the thin films was analyzed by X-ray diffraction (XRD, Philips, X'pert-PRO-MRD, Cu K $\alpha$  = 0.15405 nm, 40 kV, 30 mA) over the scan range,  $2\theta = 10\text{--}80^\circ$ . Energy-dispersive X-ray (EDX, Oxford Instruments, INCA) installed in the field emission scanning electron microscope (FESEM, JEOL, JSM-7500F) and X-ray photoelectron spectroscopy (XPS, VG Microtech, ESCA2000) were used to characterize the chemical composition ratio of Se in the as-deposited and RTA-treated thin films. XPS was equipped with a monochromatic Al K $\alpha$  X-ray source (1486.6 eV). A take-off angle of  $90^\circ$  was used for all analyses. For the high-resolution spectra, all binding energies were referenced to the C 1s peak at 285.0 eV. The optical properties of the as-deposited and RTA-treated thin films were measured using an ultraviolet-visible spectrophotometer (Varian Techtron, Cary500scan) in the range, 400–1500 nm. The electrical properties of the thin films, including the carrier concentration, resistivity and mobility were characterized using a Hall Effect measurement system (Accent Optical Technologies, HL5500PC) at room temperature.

### 3. Results and Discussion

Fig. 1 shows the XRD patterns of the (a) as-deposited and RTA-treated CIS thin films at various annealing temperatures including (b) 250°C, (c) 300°C, (d) 350°C and (e) 400°C. The XRD pattern of the as-deposited CIS thin film showed a broad and weak peak at approximately  $2\theta = 27^\circ$  corresponding to the position of the (112) peak of CIS, confirming the almost amorphous nature. No notable changes in spectra except for the broad and weak peaks were detected in the RTA-treated CIS thin films at the relatively lower temperatures  $\leq 300^\circ\text{C}$ . This means that the microstructure was amorphous. The XRD patterns became sharper / stronger after annealing at  $\geq 350^\circ\text{C}$ , indicating enhanced crystalline quality in CIS thin films. The RTA-treated CIS thin films at both 350°C and 400°C showed the major XRD peaks with preferred orientations of (112), (220) / (204) and (312) / (116) at  $2\theta = 26.59^\circ$ ,  $44.33^\circ$  and  $52.61^\circ$ , respectively, corresponding to the crystallographic planes in the CIS chalcopyrite phase [6, 12]. The peak intensity of (112) was stronger than the other peaks in the RTA-treated CIS thin films at annealing temperatures  $\geq 350^\circ\text{C}$ . This indicates that the preferential orientation of the crystallites was the (112) direction with the perpendicularity to the surface [13].

The inset in Fig. 1 shows the mean grain sizes ( $D$ ) and full width at half maximum (FWHM) of the predominant (112) diffraction peak. The mean grain sizes of the crystallites in each CIS thin film were estimated from the FWHM of the (112) diffraction peak using the Debye-Scherrer formula,  $D = 0.94\lambda / \omega \cos\theta$ , where  $\lambda$  is the

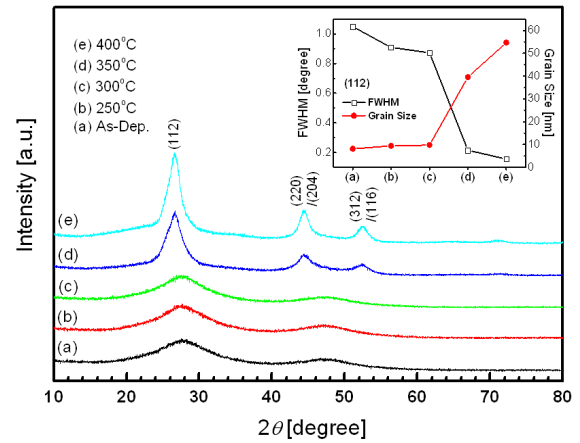


**Fig. 1.** XRD patterns of the (a) as-deposited and the RTA-treated CIS thin films at the annealing temperatures of (b) 250°C, (c) 300°C, (d) 350°C and (e) 400°C. The inset shows the FWHM of the predominant (112) diffraction peak and the grain size of the CIS thin films under the same conditions.

wavelength of K $\alpha$  radiation of Cu ( $\lambda = 0.15406$  nm),  $\omega$  is the FWHM of the (112) diffraction peak and  $\theta$  is the angle corresponding to the (112) reflection [14–16]. The FWHM of the (112) peak decreased at annealing temperatures  $\geq 350^\circ\text{C}$ , as shown in the inset in Fig. 1. This indicates that an increase in crystal quality in the CIS thin films as well as an increase in the grain size of CIS thin films along the (112) plane at an annealing temperature of approximately 350°C. The mean grain size of the as-deposited CIS thin films was approximately 8.16 nm, which increased to a maximum of 54.68 nm for the RTA-treated CIS thin films at an annealing temperature of 400°C with rapid grain growth along the (112) plane observed above 350°C [17]. Williamson and Smallman developed equations for calculating the dislocation density ( $\delta$ ), as shown in equation of  $\delta = 1 / D^2$  [18], indicating that the dislocation in the CIS thin films was reduced significantly at annealing temperatures  $\sim 350^\circ\text{C}$ .

The lattice constants,  $a$  and  $c$ , of the tetragonal structure were calculated using the equation,  $1/d^2 = (h^2 + k^2)/a^2 + l^2/c^2$ , combined with the Bragg's law,  $d = \lambda / 2\sin\theta$ , where  $d$  is the spacing between the planes in the atomic lattice (inter-planar spacing),  $hkl$  are Miller indices,  $\lambda$  is the wavelength of CuK $\alpha$  radiation ( $\lambda = 0.15406$  nm) and  $\theta$  is the angle between the incident ray and the scattering planes [19]. For a particular incident X-ray wavelength,  $\lambda$ , and the angle,  $\theta$  from XRD, the  $d$  spacing can be determined from Bragg's law. The lattice constants,  $a$  and  $c$ , can also be calculated using the (112), (220) / (204) and (312) / (116) peaks, and are represented in Fig. 2. The lattice constants,  $a$  and  $c$ , were 0.268 nm and 0.728 nm, respectively, in the as-deposited CIS thin films. These are smaller values than those of the previously published values of 0.578 nm and 1.172 nm, respectively [6, 20]. The lattice constant,  $a$ , increased slightly in the RTA-treated CIS thin films at

annealing temperatures  $\geq 350^\circ\text{C}$  and reached a maximum of 0.288 nm at  $400^\circ\text{C}$ , whereas the lattice constant,  $c$ , increased with the RTA treatment and showed a maximum of 0.776 nm at  $400^\circ\text{C}$ . The tetragonal distortion parameter,  $\eta = c/2a$ , was in the range of 1.354–1.400. This range is larger than the value of 1.003–1.008 reported for most chalcopyrite tetragonal crystals [21, 22]. A higher distortion parameter was shown in the Se-rich CIS thin films [6]. The inter-planar spacing of the (112) peak ( $d_{(112)}$ ) was also calculated using Bragg's law and is shown in Fig. 2. The  $d_{(112)}$  increased rapidly at annealing temperatures  $\geq 300^\circ\text{C}$ . The better crystallinity was obtained by a decrease in the number of crystallographic-rearrangement-induced structural defects and internal stresses [23]. This is in agreement with the grain sizes of the RTA-treated CIS thin films in the inset in Fig. 1.

Fig. 3 shows the chemical compositions of the as-deposited and RTA-treated CIS thin films with various annealing temperatures. The specimens were taken from a

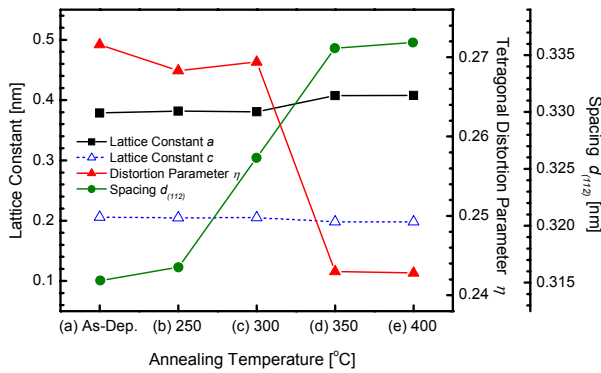


**Fig. 2.** Lattice constants ( $a$  and  $c$ ), distortion parameter  $\eta$  and inter-planar spacing  $d_{(112)}$  of the (a) as-deposited and RTA-treated CIS thin films at annealing temperatures of (b)  $250^\circ\text{C}$ , (c)  $300^\circ\text{C}$ , (d)  $350^\circ\text{C}$  and (e)  $400^\circ\text{C}$ .

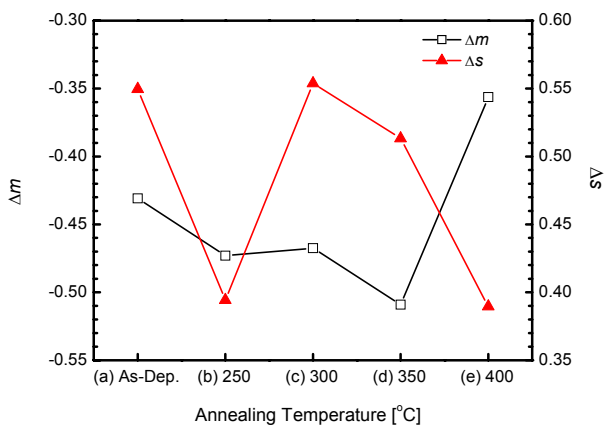


**Fig. 3.** Deviation parameters of  $\Delta m = [\text{Cu}]/[\text{In}] - 1$  and  $\Delta s = 2[\text{Se}] / ([\text{Cu}] + 3[\text{In}]) - 1$  from the chemical compositions of the (a) as-deposited and RTA-treated CIS thin films at annealing temperatures of (b)  $250^\circ\text{C}$ , (c)  $300^\circ\text{C}$ , (d)  $350^\circ\text{C}$  and (e)  $400^\circ\text{C}$  [6].

depth of 30 nm on each surface to obtain the atomic percentages of CIS thin films. The deviation from the chemical composition was used with the two parameters from the intrinsic defect model,  $\Delta m = [\text{Cu}] / [\text{In}] - 1$  and  $\Delta s = 2[\text{Se}] / ([\text{Cu}] + 3[\text{In}]) - 1$  [6]. The parameters,  $\Delta m$  and  $\Delta s$ , refer to the deviations from molecularity and valance stoichiometry, respectively. The material is stoichiometric when both parameters show no deviation. The chemical composition of the as-deposited and RTA-treated CIS thin films with various annealing temperatures was analyzed by extracting the atomic percentage of them with EDX and XPS detector units. The as-deposited CIS thin films had  $\Delta m = -0.431$  and  $\Delta s = 0.550$ . The Cu-poor ( $\Delta m < 0$ ) and Se-excess ( $\Delta s > 0$ ) composition was obtained in the as-deposited specimen. Although the deposition rates of the  $\text{CuSe}_2$  and  $\text{InSe}_2$  targets were similar, the Cu and In compositions were not identical. All specimens in this study showed a Cu-poor and Se-excess composition, but both deviations became close to '0', indicating an approach to a near-stoichiometric composition at  $400^\circ\text{C}$  in the RTA-treated CIS thin films. If the annealing temperature increased to more than  $400^\circ\text{C}$ , the Se-loss might be activated to be nearer-stoichiometric composition.

The conductivity type was determined by the deviations ( $\Delta m$  and  $\Delta s$ ) [24], which has been verified and developed the relationship further [6]. The conductivity of the CIS thin films in this study with  $\Delta m < 0$  and  $\Delta s > 0$  should have n-type conductivity, but the Hall Effect measurements showed p-type conductivity in all specimens. This was attributed to the large deviation from stoichiometry. P-type conductivity induces better electrical conductivity and higher efficiency in solar cells compared to n-type conductivity [25]. Hall Effect measurements were performed to examine the electrical properties of the as-deposited and RTA-treated CIS thin films, such as the conductivity type, carrier mobility, resistivity, and carrier concentration, as a function of the annealing temperature, as shown in Fig. 4. The carrier concentration of the as-deposited CIS thin films was in the order of  $10^{10} \text{ cm}^{-3}$  excessive holes due to p-type conductivity. This is similar or inferior to the free carrier concentration reported in intrinsic p-type CIS thin films ( $10^{10} - 10^{21} \text{ cm}^{-3}$ ) [26, 27]. The carrier concentration of the RTA-treated CIS thin films increased significantly to  $10^{13} \text{ cm}^{-3}$  at annealing temperatures  $\geq 350^\circ\text{C}$ . Twelve possible intrinsic defects can exist in CIS thin films; vacancies ( $V_{\text{Cu}}$ ,  $V_{\text{In}}$ ,  $V_{\text{Se}}$ ), interstitials ( $\text{Cu}_i$ ,  $\text{In}_i$ ,  $\text{Se}_i$ ) and anti-site defects ( $\text{Cu}_{\text{In}}$ ,  $\text{In}_{\text{Cu}}$ ,  $\text{In}_{\text{Se}}$ ,  $\text{Se}_{\text{In}}$ ,  $\text{Cu}_{\text{Se}}$ ,  $\text{Se}_{\text{Cu}}$ ) [28]. The increased carrier concentration in the CIS thin films was attributed to the reduction in  $V_{\text{Se}}$  and/or increase in the acceptor centers including  $V_{\text{Cu}}$ ,  $V_{\text{In}}$ ,  $\text{Cu}_{\text{In}}$  and  $\text{Se}_i$ . Considering the increase in Cu composition at  $400^\circ\text{C}$  in Fig. 3, the increase in  $V_{\text{In}}$  is believed to be the main contribution to the increase in carrier concentration. The increase in carrier concentration, acting as acceptors in p-type CIS thin films, can lead to a decrease in the band gap energy of CIS thin films. This

would allow more efficient harvesting of the incident light at longer wavelengths. The resistivity of the as-deposited and RTA-treated CIS thin films was in the order of 10<sup>5</sup> Ω-cm. The values (10<sup>3</sup> – 10<sup>4</sup> Ω-cm) reported in the p-type CIS thin films were similar to these values [29]. The high resistivity of the CIS thin films was attributed to the In-rich composition of CIS thin films. Highly conducting and highly resistive properties were obtained with Cu-rich and Cu-poor compositions, respectively [30]. The increase in Cu composition (Fig. 3) and the carrier concentration caused a decrease in the resistivity of the RTA-treated CIS thin films at annealing temperatures ≥ 350°C.

Fig. 5 shows the experimentally-measured optical transmittance in the visible to near-infrared (NIR) spectral region of the as-deposited and RTA-treated CIS thin films. All spectra were ≤ 42% in the visible spectral region (400 - 800 nm). The mean optical transmittance was also ≤ 8%

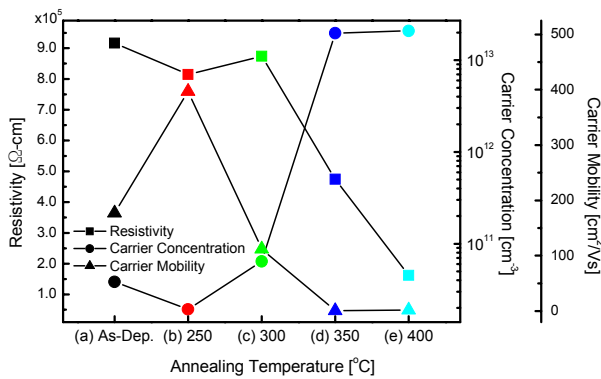


**Fig. 4.** Hall Effect measurements (carrier concentration, resistivity and carrier mobility) of the (a) as-deposited and RTA-treated CIS thin films at annealing temperatures of (b) 250°C, (c) 300°C, (d) 350°C and (e) 400°C.

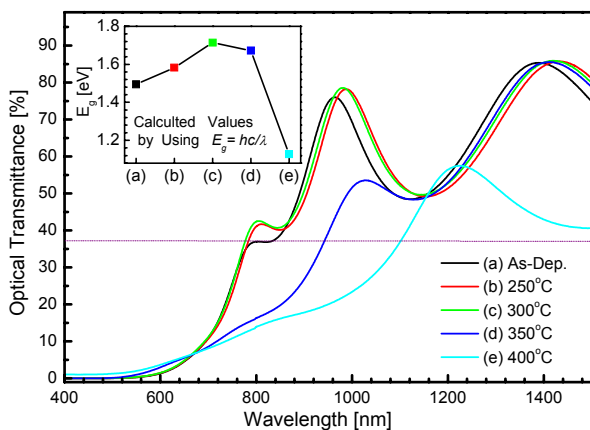


**Fig. 5.** Optical transmittance of the (a) as-deposited and the RTA-treated CIS thin films at annealing temperatures of (b) 250°C, (c) 300°C, (d) 350°C and (e) 400°C. The inset shows the calculated optical band gap energy of the CIS thin films under the same conditions.

over the same wavelength range. The mean optical transmittance of the RTA-treated CIS thin films was 4.89% and 5.01% at annealing temperatures of 350°C and 400°C, respectively. These were somewhat lower than that of the as-deposited CIS thin film (7.72%). Throughout the visible spectral region (400 - 800 nm), both the as-deposited and RTA-treated CIS thin films revealed considerable absorption because all the spectra converged to the ‘0’ value regardless of the annealing treatment. The Burstein–Moss (B–M) shift was also observed after the RTA treatment at annealing temperatures < 350°C. This is the decrease in the range of spectral transmission to the shorter solar emission spectrum in the optical transmittance, highlighting the advantages of CIS thin films as the absorber layer in thin film photovoltaic devices due to the shift of the absorption edge to a larger wavelength in absorption coefficient ( $\alpha$ ) [31-33]. When the wavelength range was widened from visible spectral region to the NIR spectral region (400-1500 nm), the mean optical transmittance of the RTA-treated CIS thin films at the annealing temperatures of 350°C and 400°C increased gradually to 36.89% and 25.18%, respectively. That of the as-deposited and RTA-treated CIS thin films annealed at ≤ 250°C increased rapidly to 43.09–43.80% over the same spectral range. The equation,  $E_g = hc/\lambda$ , was used to calculate the optical band gap energies of the CIS thin films with the same thickness (530 nm), where  $h$  is Planck’s constant ( $4.135667 \times 10^{-15}$  eVs),  $c$  is the velocity of light ( $3 \times 10^8$  m/s) and  $\lambda$  is the wavelength (nm) of the absorption onset ( $1/e = 37\%$ ). The optical band gap energy ( $E_g$ ) of the as-deposited and RTA-treated CIS thin films at annealing temperatures of 250°C, 300°C, 350°C and 400°C were 1.495 eV, 1.583 eV, 1.714 eV, 1.672 eV and 1.127 eV, respectively, as shown in the inset in Fig. 5. This is inversely proportional to the deviation parameter,  $\Delta m$ , in Fig. 3. The decreased optical band gap energy at annealing temperatures of 400°C was attributed to the increased grain size (Fig. 1), decreased In composition (Fig. 2), increased spacing  $d$  (better crystallinity) (Fig. 3) and increased carrier concentration (Fig. 4). This is attributed to both crystallinity and intrinsic defects that cause a shift in the absorption edge followed by the RTA treatment [17, 34]. An increase in grain size leads to a decrease in the optical band gap energy due to the fewer free carrier concentrations and lower potential barriers originating from large particles with fewer grain boundaries and imperfections [35].

#### 4. Conclusion

A co-sputtering process for preparing CIS thin films was advanced by using a CuSe<sub>2</sub> and InSe<sub>2</sub> targets without a Se- / S-containing gas in the RTA treatment by a function of the annealing temperature. The grains grew along the predominant (112) plane in the RTA-treated CIS thin

films at annealing temperatures  $\geq 350^\circ\text{C}$ . The mean grain size of approximately 8.16 nm for the as-deposited CIS thin films increased to a maximum of 54.68 nm for the RTA-treated CIS thin films at an annealing temperature of  $400^\circ\text{C}$ . This suggests that the dislocation was reduced noticeably after annealing at  $\sim 350^\circ\text{C}$ , which was confirmed by the distortion parameter  $\eta$ . The inter-planar spacing  $d_{(112)}$  increased after annealing at  $\geq 300^\circ\text{C}$ . This means that the crystallinity became improved. Despite the same deposition rates of each target in the co-sputtering process, a Cu-poor ( $\Delta m < 0$ ) and Se-excess ( $\Delta s > 0$ ) composition was obtained in the as-deposited specimen. The RTA-treated CIS thin films approached to the near-stoichiometric composition at the temperature of  $400^\circ\text{C}$ . The carrier concentration of the RTA-treated CIS thin films increased significantly from  $10^{10} \text{ cm}^{-3}$  to  $10^{13} \text{ cm}^{-3}$  after annealing at  $\geq 350^\circ\text{C}$ . The resistivity of the as-deposited CIS thin films was in the order of  $10^5 \Omega\text{-cm}$  due to the In-rich composition. It decreased with increasing Cu composition and carrier concentration at annealing temperatures of  $\geq 350^\circ\text{C}$ . The mean optical transmittance of the RTA-treated CIS thin films at annealing temperature of  $400^\circ\text{C}$  was 25.18%, whereas that of the as-deposited CIS thin films was 43.29% in the spectral range of 400 - 1500 nm. The optical band gap energy ( $E_g$ ) of the CIS thin films showed an opposite tendency to the deviation parameter  $\Delta m$ . It decreased from 1.495 eV (as-deposited) to 1.127 eV (RTA-treated at  $400^\circ\text{C}$ ) due to the increase in grain size, inter-planar spacing and carrier concentration as well as the decrease in In composition. The decreased optical band gap energy would allow the absorption of more incident-light at longer wavelengths.

### Acknowledgements

This research was financially supported by the Ministry of Education, Science Technology (MEST) and National Research Foundation of Korea (NRF) through the Human Resource Training Project for Regional Innovation.

### References

- [1] I. H. Choi, "The Preparation of CIS Absorber Layers by Using MOCVD with Two Different Methods," *Journal of the Korean Physical Society*, Vol. 59, No. 1, July 2011, pp. 80-84.
- [2] M. Varela, E. Bertran, M. Manchon, J. Esteve and J. L. Morenza, "Optical properties of co-evaporated CuInSe, thin films," *Journal of Physics D: Applied Physics*, Vol. 19, No. 1, 1986, pp. 127-136.
- [3] M. A. S. Bhuiyan, A. S. Bhuiyan, A. Hossain and Z. H. Mahmood, "Studies on optical characteristics of CuInSe<sub>2</sub> thin films," *Central European Journal of Engineering*, June 2013, Vol. 3, No. 2, pp. 170-173.
- [4] O. Schultz, S.W. Glunz and G.P. Willeke, "Multicrystalline silicon solar cells exceeding 20% efficiency," *Progress in Photovoltaics: Research and Applications*, Vol. 12, No. 7, 2004, pp. 553-558.
- [5] Y. C. Lin, Z. Q. Lin, C. H. Shen, L. Q. Wang, C. T. Ha and C. Peng, "Cu(In, Ga)Se<sub>2</sub> films prepared by sputtering with a chalcopyrite Cu(In,Ga)Se<sub>2</sub> quaternary alloy and In targets," *Journal of Materials Science: Materials in Electronics*, Vol. 23, No. 2, 2012, pp. 493-500.
- [6] S. Karthikeyan, A. E. Hill, R. D. Pilkington, J. S. Cowpe, J. Hisek and D. M. Bagnall, "Single step deposition method for nearly stoichiometric CuInSe<sub>2</sub> thin films," *Thin Solid Films* Vol. 519, 2011, pp. 3107-3112.
- [7] B. T. Jheng, P. T. Liu, M. C. Wu and H. P. D. Shieh, "A non-selenization technology by co-sputtering deposition for solar cell applications," *Optics Letters*, Vol. 37, No. 13, 2012, pp. 2760-2762.
- [8] D. Chen and D. Wang, "Formation of CuInSe<sub>2</sub> from Cu<sub>2</sub>Se and In<sub>2</sub>Se<sub>3</sub> compounds," *Phys. Status Solidi A*, Vol. 208, No. 10, 2011, pp. 2415-2423.
- [9] K. Bouabid, A. Ihlal, A. Manar, A. Outzourhit and E. L. Ameziane, "Effect of deposition and annealing parameters on the properties of electrodeposited CuIn<sub>1-x</sub>Ga<sub>x</sub>Se<sub>2</sub> thin films," *Thin Solid Films*, Vol. 488, 2005, pp. 62-67.
- [10] E. Ahmed, A. Zegadi, A. E. Hill, R. D. Pilkington, R. D. Tomlinson, A. A. Dost, W. Ahmed, S. Leppävuori, J. Levoska and O. Kusmartseva, "The influence of annealing processes on the structural, compositional and electro-optical properties of CuIn<sub>0.75</sub>Ga<sub>0.25</sub>Se<sub>2</sub> thin films," *Journal of Materials Science: Materials in Electronics*, Vol. 7, No. 3, 1996, pp. 213-219.
- [11] X. Wang, S. S. Li, W. K. Kim, S. Yoon, V. Craciun, J. M. Howard, S. Easwaran, O. Manasreh, O. D. Crisalle and T. J. Anderson, "Investigation of rapid thermal annealing on Cu(In, Ga)Se<sub>2</sub> films and solar cells," *Solar Energy Materials and Solar Cells*, Vol. 90, No. 17, 2006, pp. 2855-2866.
- [12] F. O. Adurodija, J. Song, S. D. Kim, S. H. Kwon, S. K. Kim, K. H. Yoon and B. T. Ahn, "Growth of CuInSe<sub>2</sub> thin films by high vapour Se treatment of co-sputtered Cu-In alloy in a graphite container," *Thin Solid Films*, Vol. 338, 1999, pp. 13-19.
- [13] S. Phok, S. Rajaputra and V. P. Singh, "Copper indium diselenide nanowire arrays by electrodeposition in porous alumina templates," *Nanotechnology*, Vol. 18, No. 47, 2007, p. 475601.
- [14] J. C. Osuwa and N. I. Chigbo, "Effects of temporal variations in deposition on the optical and solid state properties of electro-deposited cadmium telluride (CdTe) thin films on glass FTO," *Chalcogenide Lett.*, Vol. 9, No. 12, 2012, pp. 501-508.
- [15] B. D. Cullity, *Elements of X-Ray Diffraction*, 3rd ed. Addison-Wesley, Reading, Mass., London, 1967.

- [16] G. Gordillo, J. M. Flórez and L. C. Hernández, "Preparation and characterization of CdTe thin films deposited by CSS," *Solar Energy Materials and Solar Cells*, Vol. 37, No. 3-4, 1995, pp. 273-281.
- [17] N. H. Kim, C. I. Park, J. Park, "A Pilot Investigation on Laser Annealing for Thin-film Solar Cells: Crystallinity and Optical Properties of Laser-annealed CdTe Thin Films by Using an 808-nm Diode Laser," *Journal of the Korean Physical Society*, Vol. 62, No. 3, 2013, pp. 502-507.
- [18] G. K. Williamson, R. E. Smallman, "Dislocation densities in some annealed and cold-worked metals from measurements on the x-ray Debye-Scherrer spectrum," *Philosophical Magazine*, Vol. 1, No. 1, 1956, pp. 34-45.
- [19] M. A. Islam, Q. Huda, M. S. Hossain, M. M. Aliyu, M. R. Karim, K. Sopian, N. Amin, "High quality 1 μm thick CdTe absorber layers grown by magnetron sputtering for solar cell application," *Current Applied Physics*, Vol. 13, Suppl. 2, 2013, pp. S115-S121.
- [20] L. L. Kazmerski, O. Jamjoum, P. J. Ireland, S. K. Deb, R. A. Mickelsen and W. Chen, "Initial oxidation of CuInSe<sub>2</sub>," *Journal of Vacuum Science and Technology*, Vol. 19, No. 3, 1981, pp. 467-471.
- [21] M. L. Fearheiley, K. J. Bachmann, Y. H. Shing, S. A. Vasquez and C. R. Herrington, "The lattice constants of CuInSe<sub>2</sub>," *Journal of Electronic Materials*, Vol. 14, No. 6, 1985, pp. 677-683.
- [22] A. A. I. Al-Bassam and U. A. Elani, Proceeding of 2012 International Conference on Environment, Energy and Biotechnology, IPCBEE Vol. 33, IACSUT Press, Singapore, 2012, pp. 163-167.
- [23] A. Bouraiou, M. S. Aida, A. Mosbah, and N. Attaf, "Annealing time effect on the properties of CuInSe<sub>2</sub> grown by electrodeposition using two electrodes system," *Brazilian Journal of Physics*, Vol. 39, No. 3, 2009, pp. 543-546.
- [24] H. Neumann and R.D. Tomlinson, "Relation between electrical properties and composition in CuInSe<sub>2</sub> single crystals," *Solar Cells*, Vol. 28, No. 4, 1990, pp. 301-313.
- [25] D. Haneman, "Properties and applications of copper indium diselenide," *Critical Reviews in Solid State and Materials Sciences*, Vol. 14, No. 4, 1988, pp. 377-413
- [26] R. Chen and C. Persson, "Band-edge density-of-states and carrier concentrations in intrinsic and p-type CuIn<sub>1-x</sub>Ga<sub>x</sub>Se<sub>2</sub>," *Journal of Applied Physics*, Vol. 112, No. 10, 2012, p. 103708.
- [27] G. A. Medvedkin and M. A. Magomedov, "Growth of polycrystalline CuInSe<sub>2</sub> thin films by effusion evaporation," *Semiconductor Science and Technology*, Vol. 8, No. 5, 1993, pp. 652-656.
- [28] S. R. Kodigala, Cu(In<sub>1-x</sub>Ga<sub>x</sub>)Se<sub>2</sub> Based Thin Film Solar Cells, Vol. 35, Academic Press, MA, USA, 2011, p. 215.
- [29] A. Knowles, H. Oumous. M. J. Carter and R. Hill, Conference Record of the Twentieth IEEE Photovoltaic Specialists Conference, Vol. 2, IEEE, Las Vegas, NV, USA, 1988, p. 1482.
- [30] T. Datta, R. Noufi and S. K. Deb, "Electrical conductivity of p-type CuInSe<sub>2</sub> thin films," *Applied Physics Letters*, Vol. 47, No. 10, 1985, pp. 1102-1104.
- [31] H. Khallaf, G. Chai, O. Lupan, L. Chow, S. Park and A. Schulte, "Characterization of gallium-doped CdS thin films grown by chemical bath deposition," *Applied Surface Science*, Vol. 255, No. 7, 2009, pp. 4129-4134.
- [32] D. S. Reddy, K. N. Rao, K. R. Gunasekhar, N. K. Reddy, K. S. Kumar and P. S. Reddy, "Annealing effect on structural and electrical properties of thermally evaporated Cd<sub>1-x</sub>Mn<sub>x</sub>S nanocrystalline films," *Materials Research Bulletin*, Vol. 43, No. 12, 2008, pp. 3245-3251.
- [33] Y. Gu, X. Li, W. Yu, X. Gao, J. Zhao and C. Yang, "Microstructures, electrical and optical characteristics of ZnO thin films by oxygen plasma-assisted pulsed laser deposition," *Journal of Crystal Growth*, Vol. 305, No. 1, 2007, pp. 36-39.
- [34] S. Wageh, A. A. Higazy and M. A. Algradee, "Optical Properties and Activation Energy of A Novel System of CdTe Nanoparticles Embedded in Phosphate Glass Matrix," *Journal of Modern Physics*, Vol. 2, No. 8, 2011, pp. 913-921.
- [35] C. V. Ramana, R. J. Smith and O. M. Hussain, "Grain size effects on the optical characteristics of pulsed-laser deposited vanadium oxide thin films," *Physica Status Solidi A*, Vol. 199, No. 1, 2003, pp. R4-R6.



**Nam-Hoon Kim** He received the B.S., M.S. and Ph.D. degrees in Electrical Engineering from Chung-Ang University, Seoul, Korea in 1997, 1999 and 2004, respectively. He continued his researches as a Research Professor at Chosun University, Sungkyunkwan University and Chonnam National University, Korea during 2004-2010. Since September 2010, he has been with the faculty as an Assistant Professor at the Department of Electrical Engineering, Chosun University, Gwangju, Korea. His research interests include nonvolatile memory devices, heterostructured thin-film photovoltaic cells, printable electronic devices, micro-nanofabricated batteries, and their manufacturing processes.



**Young-Kil Jun** He received the B.S. and M.S. degrees in Electrical Engineering from Chosun University, Gwangju, Korea in 2006 and 2008, respectively. He is currently working toward the Ph.D. degree at Chosun University. His current research interests include low-cost / high-efficiency

thin-film solar cells and batteries for electric vehicle (EV).



**Geum-Bae Cho** He was born in Chonnam, Korea, in 1954. He received the B.S. and M.S degrees in Electrical Engineering from Chosun University, Gwangju, Korea in 1980 and 1982, respectively, and the Ph.D. degree from Konkuk University, Seoul, Korea in 1995. Since 1985, he has been a Professor at the Department of Electrical Engineering, Chosun University, where he is currently the Director of the Engineering Technology Institute of Chosun University. He has authored or co-authored more than 100 published technical papers. His research interests include power electronics, analysis and control of motor, and power converter for photovoltaic power system. Prof. Cho served as the Vice-President of the Korea Institute of Power Electronics (KIPE) in 2008 and the Korean Institute of Electrical Engineers (KIEE) during 2012-2013. He has been engaged in various academic societies such as the KIPE, the KIEE, and the Korean Solar Energy Society.